



## Implications for magmatic processes at Ontong Java Plateau from volatile and major element contents of Cretaceous basalt glasses

Peter J. Michael

*Department of Geosciences, University of Tulsa, 600 South College Avenue, Tulsa, Oklahoma 74104  
(pjm@utulsa.edu)*

**Abstract.** [1] Major elements Cl, CO<sub>2</sub>, and H<sub>2</sub>O were determined in unaltered tholeiitic basalt glasses from Drilling Program Sites 803D and 807C on Ontong Java Plateau (OJP), and Sites 462A in Nauru Basin (NB) and 802A in East Mariana Basin (EMB). Glasses are moderately evolved (Mg# = 5360) with low Na<sub>2</sub>O, indicating they formed by large extents of melting. Extent of melting is less for glasses from OJP than from EMB, requiring faster or more focused mantle upwelling or a longer period of activity for OJP. Glasses within each hole define 13 different compositional types. Each compositional type is made up of many glass-bounded flow units whose chemistry is identical within analytical uncertainty, suggesting that each compositional type formed during a single eruptive episode with multiple magma surges. The lack of diversity within each type also suggests that the magmatic system was large and well buffered. Major element chemistry also requires that significant shallow crystallization occurred during plateau formation and limits the amount of deep crystallization that might be responsible for the thick crust of the plateau. Chlorine contents are constant within each compositional type and are 580 ppm in type A and 850 ppm in types CG from Hole 807C, and 360 ppm in glasses from Hole 803D. Glasses from 802A and 462A have ~240 ppm and 1975 ppm Cl, respectively. Cl/K ratios range from 0.2 to 2.33, well above mid-ocean ridge basalt (MORB) mantle values (0.07), suggesting that most liquids assimilated hydrothermally altered material as they ascended and crystallized. High Cl/K ratios also suggest that abundant hydrothermal activity may have accompanied plateau formation. Low dissolved CO<sub>2</sub> (i.e., CO<sub>3</sub><sup>2-</sup>) contents in one OJP compositional type (54 ppm in 807C type A) are similar to those on shallow sections of the mid-ocean ridge and are consistent with a maximum depth of eruption of 1320 ± 250 m, in contrast to the greater eruption depths inferred from fossils in the overlying sediments. Our proposed eruption depth falls in the MORB field on a plot of depth versus Na<sub>8,0</sub> supporting a ridge or near-ridge origin. The shallow depth estimate allows for more postformation subsidence and diminishes the importance but does not eliminate the need for additional processes such as prolonged underplating to account for OJP's shallow depth. Higher CO<sub>2</sub> in other glasses, including types CG from Hole 807C, suggests that some liquids were oversaturated with CO<sub>2</sub> when emplaced and therefore did not travel far from their point of eruption. H<sub>2</sub>O contents are similar to MORB and range from 0.13 wt% for NB, to 0.25 wt% (807C, types CG) to 0.49 wt% (807C type A). Ratios of H<sub>2</sub>O to rare earth elements (REE) are slightly higher than most MORB and are similar to those from northern Mid-Atlantic Ridge (MAR), which has distinctively high H<sub>2</sub>O. H<sub>2</sub>O/Ce (constant in depleted through enriched MORB) ranges from 200 to 400, compared to 220380 for northern MAR glasses and 150250 for MORB elsewhere and >500 for arc-related glasses. The slightly higher H<sub>2</sub>O contents in the OJP mantle source could have contributed very little to the extensive melting that built the plateau, so a substantial temperature anomaly is still required.

**Keywords:** Ontong Java Plateau; basalt volatiles; magmatic processes.

**Index terms:** Minor and trace element composition; major element composition; composition of the crust; mid-ocean ridge processes.

**Received** October 25, 1999; **Accepted** October 26, 1999; **Published** December 13, 1999.

Michael, P. J., 1999. Implications for magmatic processes at Ontong Java Plateau from volatile and major element contents of Cretaceous basalt glasses, *Geochem. Geophys. Geosyst.*, vol. 1, Paper number 1999GC000025 [10,170 words, 6 figures, 2 tables]. Dec. 13, 1999.

### 1. Introduction

[2] Large igneous provinces (LIPs) are huge outpourings of basalt that are among the most prominent geological features in the world. Geochronological studies [Mahoney *et al.*, 1993a; Tarduno *et al.*, 1991] indicate that LIPs formed very rapidly and thus may have

had profound impacts on global geology, climate, and biology [Larson, 1991]. There is growing consensus from geochemical and geochronological studies [Mahoney, 1987], as well as laboratory and numerical modeling [White and Mackenzie, 1995; Campbell and Griffiths, 1990], that LIPs form when the large inflated head of mantle plume, initiated as a boundary layer

instability, intersects the lithosphere.

[3] Ontong Java Plateau (OJP) is the largest LIP. Because it is submarine and covered by sediments, very little is known about the processes attending its formation. However, analysis of basement samples of OJP from drill cores [Mahoney *et al.*, 1993a] and from upthrust subaerial parts of the plateau [Tejada *et al.*, 1996; Neal *et al.*, 1997] has improved the understanding of OJP. Unlike continental flood basalts these samples have not been influenced by transport through reactive continental crust and can provide unambiguous information about the mantle source and melting characteristics. Geochemical studies of OJP lavas show that they formed by large extents of melting of plume-like mantle [Mahoney *et al.*, 1993a]. The lavas underwent extensive crystal fractionation, suggesting that much of OJP's >30-km-thick foundation is plutonic in character [Neal *et al.*, 1997].

[4] In this work, major elements and volatile contents in fresh glasses from OJP and nearby basins were determined to further explore how this LIP was generated. Knowledge of the liquid composition permits better comparisons of source chemistry, extent of melting, and depths and extents of crystallization between sites and with modern basalts. Crystallization depths provide some limits on the amount of magmatic underplating that might have occurred during plateau formation. Cl contents and Cl/K ratios show whether magmas interacted with the crust during their ascent and also provide insight as to whether shallow magma chambers and hydrothermal systems were associated with volcanism. Concentrations of CO<sub>2</sub> that are dissolved in glasses were determined to estimate the maximum eruption depths. This information is used to constrain the subsidence history of the plateau which is important in determining if volcanism occurred in a single short episode or whether there was prolonged underplating [Ito and Clift, 1998]. Knowledge of the depths of eruption also helps us to understand whether OJP was formed as a near-ridge plume like Iceland or erupted far from a ridge [Coffin and Gahagan, 1995]. H<sub>2</sub>O contents in the glasses were measured to estimate H<sub>2</sub>O contents of the mantle sources and to speculate about the importance of H<sub>2</sub>O in promoting the extensive melting that formed OJP. Along with major and trace elements this helps to constrain melting temperatures and the magnitude of the temperature anomaly: How different is OJP from modern plumes? Are high temperatures and a plume head required? H<sub>2</sub>O/rare earth elements (REE) ratios are also used to compare

OJP's mantle source with sources of other submarine basalts.

## 2. General Features and Tectonic Setting of Ontong Java Plateau

[5] OJP is made up of a basement of Cretaceous tholeiitic basalts [Kroenke *et al.*, 1991] that is overlain by Cretaceous to modern pelagic sediments (> 1000 m thick in places). Its shallowest part lies at 1700-m depth, but most of the plateau is at 2000-3000 m depth and stands roughly 2000-3000 m above the surrounding sea-floor [Kroenke, 1972]. The southern and southwestern edges have collided with the Solomon Islands arc and are exposed above sea level in Malaita, Santa Isabel, and other islands [Tejada *et al.*, 1996; Neal *et al.*, 1997]. Estimates of crustal thickness vary widely, but recent studies [Gladczenko *et al.*, 1997] suggest that the depth to the MOHO is 3032 km, that the plateau-generated crust is up to 26 km thick, and that OJP's volume is between 44 and 56 x 10<sup>6</sup> km<sup>3</sup> [Coffin and Eldholm, 1994].

[6] Paleontologic and paleomagnetic data [Tarduno *et al.*, 1991] as well as <sup>40</sup>Ar/<sup>39</sup>Ar ages of basalts from widely separated parts of the plateau (Ocean Drilling Project, ODP, Hole 807; Deep Sea Drilling Program, DSDP, Hole 289; Santa Isabel Island and Malaita Island; see Figure 1) [Mahoney *et al.*, 1993a; Tejada *et al.*, 1996] indicate that plateau-forming eruptions ended simultaneously over areas that are up to 1600 km away and suggest that volcanism occurred over a short time interval ~122 ± 3 Ma. A second, less voluminous, interval of volcanism occurred around 90 ± 4 Ma and is represented by basalts from Hole 803D and Santa Isabel Island (Figure 1) [Mahoney *et al.*, 1993a; Tejada *et al.*, 1996]. Volcanic events recorded in basins proximal to OJP and at distant reference sites suggest a short duration and therefore a very high rate of volcanic output [Tarduno *et al.*, 1991] at 122 Ma. The initiation of what is now the Louisville hotspot may have triggered OJP's construction [Tarduno *et al.*, 1991; Mahoney and Spencer, 1991; Richards *et al.*, 1991], although there are inconsistencies with this theory [Neal *et al.*, 1997]. Despite the strength of the evidence supporting a plume head origin for OJP, special models such as nearly zero absolute plate motion from 125 to 90 Ma or a double plume head [Bercovici and Mahoney, 1994] are required to account for the later phase of volcanism (i.e., 90 Ma) of essentially identical chemical character and the apparent lack of a hotspot track.

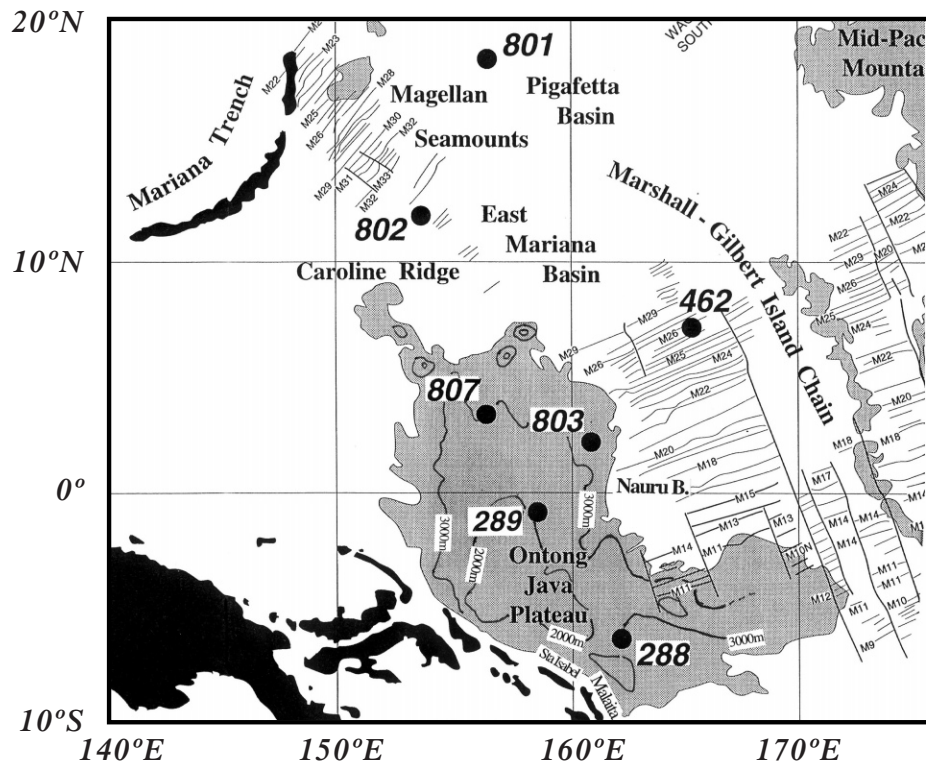


**Figure 1.** Ontong Java Plateau and surrounding basins and islands, modified from Castillo et al. [1994]. Large numbers are Deep Sea Drilling Project (DSDP) and Ocean Drilling Project drill sites. Additional samples are from Malaita Island. Approximate contours of 2000- and 3000-m depth on Ontong Java Plateau are adapted from Mahoney et al. [1993a]. The gray pattern roughly outlines the 4000-m isobath, except on the southwest side, where the plateau is uplifted.

[7] It is not known how close OJP formed to a mid-ocean ridge (MOR) [Coffin and Gahagan, 1995]. Basalt chemistry suggests that extents of melting were similar to those beneath Iceland [Mahoney et al., 1993a], the site of a ridge-centered mantle plume. However, the 2000-3000 m water depth inferred for emplacement of OJP lavas [Sliter and Leckie, 1993; Saunders et al., 1994] is inconsistent with the modern relationship between vigorous ridge-centered plumes and depth on the MOR. The new estimates of eruption depth herein therefore have some bearing on this question. Diverse evidence "weighs lightly against" the generation of OJP at a mid-ocean ridge similar to Iceland [Coffin and Gahagan, 1995]. Extrapolation of magnetic anomalies from the surrounding seafloor suggests that OJP was emplaced on crust that ranged from 9 to 28 Myr old [Gladchenko et al., 1997]. A plume head responsible for OJP may have eventually become associated with a nearby ridge axis through its influence

on ridge propagation [Mahoney et al., 1993a; Mahoney and Spencer, 1991], and this might account for the similarity of basalts' major elements with those of Iceland or Kolbeinsey Ridge (Figure 2). This might also account for the lack of a hotspot track. All of the lavas collected thus far from OJP, EMB, and NB underwent extensive fractional crystallization, possibly from picritic or komatiitic primary magmas [Neal et al., 1997; Storey et al., 1991].

[8] Basalts that are very similar in age and chemical and isotopic composition to those from OJP were recovered from EMB to the north of OJP and NB to the east of OJP, at ODP Hole 802A and DSDP Hole 462A, respectively (Figure 1) [Castillo et al., 1986]. EMB basalts are dated at  $114.6 \pm 3.2$  Ma [Castillo et al., 1994], while those of NB yielded ages of  $110.8 \pm 1.0$  Ma [Castillo et al., 1991]. These ages are within error of each other and are consistent with ages of overlying sediments but younger than the Jurassic ages predicted

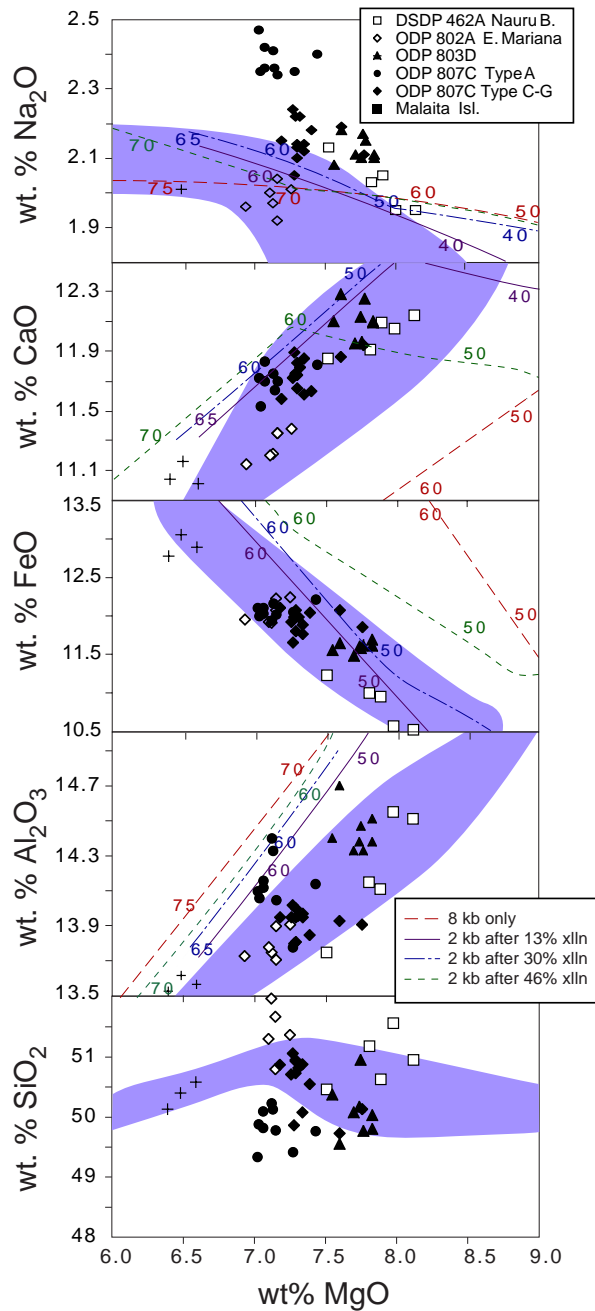


**Figure 2.** Major element chemistry of basalt glasses. The very thin (magenta) lines outline the fields of mid-ocean ridge basalt (MORB) from Kolbeinsey Ridge [Devey et al., 1994] for comparison. The scatter for each symbol mostly reflects analytical uncertainty. Only the symbols for DSDP 462A show compositional diversity that is significantly greater than analytical uncertainty and appear to define trends. The overall pattern displayed by the different sample types reflects varying extents of

fractional crystallization of parental magmas that were broadly similar in composition. Lines show expected trends of liquids derived by fractional crystallization using the model of Weaver and Langmuir [1980]. Numbered ticks on the lines correspond to the percent crystallized from an initial picritic liquid with 16.25% MgO, 47.8% SiO<sub>2</sub>, 0.6% TiO<sub>2</sub>, 14% Al<sub>2</sub>O<sub>3</sub>, 8.5% FeO, 11% CaO, and 1.4% Na<sub>2</sub>O. Besides being run entirely at 8 kbar, the model was run with 13%, 30%, 46% crystallization occurring at 8 kbar, followed by additional crystallization at 2 kbar. (The trend for crystallization at 2 kb-only is the same as the trend for 13% crystallization at 8 kbar, because both involve OL-only crystallization.) The primary liquid and high-MgO parts of the trends are not shown because they would render the rest of the diagram too small. Note that the high SiO<sub>2</sub> and CaO and low FeO of the glasses require that they could not have more than ~30-40% crystallization at 8 kbar, before ascending to shallower depths and crystallizing further. Na<sub>2</sub>O was not plotted for two Malaita glasses because they were so low, probably because of alteration.

by extrapolation of marine magnetic anomalies into the basins. The basalts were probably formed during Cretaceous rifting of earlier Jurassic basins that was related to the formation of OJP [Castillo et al., 1994], and may have occurred at a MOR.

### 3. Samples

[9] Glass intervals were sampled from cores to obtain the freshest, most crystal-free and most representative material possible from each core. Hole 289 contained no glass suitable for analysis. Previous studies [Castillo et al., 1991, 1994; Mahoney et al., 1993b; Batiza, 1981; Saunders, 1986] that identified different chemical types were used as guides. Sample material that was left over from these studies was also analyzed.

[10] All of the basalts are fine-grained tholeiites and are crystal-poor to aphyric. Vesicles are rare or absent. Glasses are slightly to mostly altered to clays or palagonite. Transparent wafers show 100-1000 μm zones of glass that are completely free of alteration. Most analyzed glasses were free of crystals and microlites, but a few had scattered microlites because no better material was available from certain parts of the cores. Three glasses from Malaita were also analyzed [Tejada et al., 1996; Neal et al., 1997]. They are similar to the type A of Hole 807C. Their color and H<sub>2</sub>O contents suggest that they have suffered alteration, even though their major element chemistry was consistent with mag-



matic values.

## 4. Analytical Methods

[11] The freshest and clearest glass shards available were mounted in Buehler Transoptic® and then ground and polished on both sides to a thickness suitable for analysis by Fourier transform infrared (FTIR) spectroscopy: 50200  $\mu\text{m}$ . While still mounted, the transparent glass wafers were analyzed by electron microprobe for major elements Cl and K. The transparency of the wafers allowed us to avoid areas of alteration. Major elements Cl and K were determined using the Cameca MBX electron microprobe at the University of Tulsa following the methods described earlier *Michael et al.*, 1989; *Michael and Cornell*, 1998]. Cl and K were counted for 30 min per sample to obtain a reproducibility of about  $\pm 20$  ppm Cl or K at a concentration of 400 ppm.

[12] After microprobe analysis the wafers were dismounted and cleaned with acetone and then mapped for thickness ( $\pm 1$   $\mu\text{m}$  precision) using a digital micrometer. Concentrations of volatiles dissolved in glasses (not in vesicles), including  $\text{CO}_3^{2-}$ , molecular  $\text{CO}_2$ , molecular  $\text{H}_2\text{O}$  ( $\text{H}_2\text{O}_M$ ), and  $\text{OH}^-$ , were analyzed by FTIR at the University of Tulsa, using published methods and calibrations [*Dixon et al.*, 1988; 1995] with slight modifications [*Michael*, 1995].  $\text{CO}_3^{2-}$  appears as an absorbance doublet at 1435 and 1515  $\text{cm}^{-1}$  [*Fine and Stolper*, 1986]. Estimation of the complex background in this region is often the largest source of analytical error, so the spectrum of a volatile-free reference glass from Juan de Fuca Ridge [*Dixon et al.*, 1988] was subtracted from each sample spectrum and the background of the resulting spectrum was determined following published methods closely [*Dixon et al.*, 1988, 1995; *J. Dixon*, personal communication, 1998]. Since the solubility versus pressure determinations were done using this method [*Dixon et al.*, 1995], this ensures that our depth constraints will be as accurate as possible. Concentrations are reproducible to better than  $\pm 20\%$  of the amount present. The presence of microlites and devitrification may influence  $\text{CO}_2$  abundances [*Dixon et al.*, 1988]. No significant differences in  $\text{CO}_2$  were noted between glasses with microlites and those with none. Replicate analyses of  $\text{H}_2\text{O}$  in different wafers from the same specimen were reproducible to  $\pm 5\%$ . A few samples with  $\text{H}_2\text{O} < 0.2\%$  were reproducible to  $\pm 15\%$  of the amount present. Replicate analyses of the same 80  $\mu\text{m}$  spot were closer:  $\pm 3\%$ .

[13] The new analyses of glasses (Table 1) are similar to the published analyses of whole-rock powders [*Mahoney et al.*, 1993a; *Tejada et al.*, 1996; *Neal et al.*, 1997, *Castillo et al.*, 1991, 1994] that showed that the lavas are all tholeiitic and are fairly evolved and have low  $\text{Na}_2\text{O}$  and very high FeO (Figure 2) indicative of large extents of partial melting and a large average depth of melting [*Mahoney et al.*, 1993a; *Langmuir et al.*, 1992]. The glasses are similar to MORB from Kolbeinsey Ridge (Figure 2). The glass analyses confirm earlier proposals [*Mahoney et al.*, 1993a, b] that there are two different chemical types in Hole 807C: type A (upper) with higher  $\text{Na}_2\text{O}$ ,  $\text{K}_2\text{O}$ ,  $\text{TiO}_2$ , and  $\text{Al}_2\text{O}_3$  and types CG (lower) with higher  $\text{SiO}_2$  and MgO. Each chemical type comprises many different cooling units. A similar arrangement with three chemical types was described for Hole 462A [*Saunders*, 1986], but our glass analyses suggest that their middle type is made up of three chemical types that differ slightly in their degree of evolution. These are so close in composition that they are not discernible in the figures. Glasses 462A-47R-2 and 462A-47R-3 are the first type. Glasses 462A-51R-4 and 462A-56R-1 are a second type, and the single glass from 462A-69R-1 is a third type. No glasses were found or analyzed in the upper and lower chemical types of Hole 462A defined by *Saunders* [1986]. The glass data confirm earlier studies that showed Holes 802A and 803D each contain one chemical type. The glass data are unaffected by crystal accumulation and alteration and show that all of the flows within a chemical type, which may be  $>50$  m thick and comprise 50 different flows, have nearly identical chemistry within analytical error. This is also true for the precise analyses of Cl and K. This remarkable interflow homogeneity is discussed further in section 6.1.1. It is also remarkable how small the range of evolution is within each site and between all of the sites: Mg# ranges from 53 to 60, and K/Ti ranges from 0.13 to 0.18 (Figure 3) for the four different holes (seven chemical types) studied.

## 5. Results

### 5.1. Major Elements

[14] The variations in glass chemistry displayed by the eight different chemical types plus Malaita (Figure 2: increasing FeO,  $\text{Na}_2\text{O}$ ,  $\text{K}_2\text{O}$ , and  $\text{TiO}_2$  and decreasing CaO and  $\text{Al}_2\text{O}_3$  with decreasing MgO) are consistent with variable extents of fractionation of parental picritic or tholeiitic liquids that were broadly similar



**Table 1. Chemistry and Crystallization Pressures of Glasses From Nauru Basin, Ontong Java Plateau, and East Mariana**

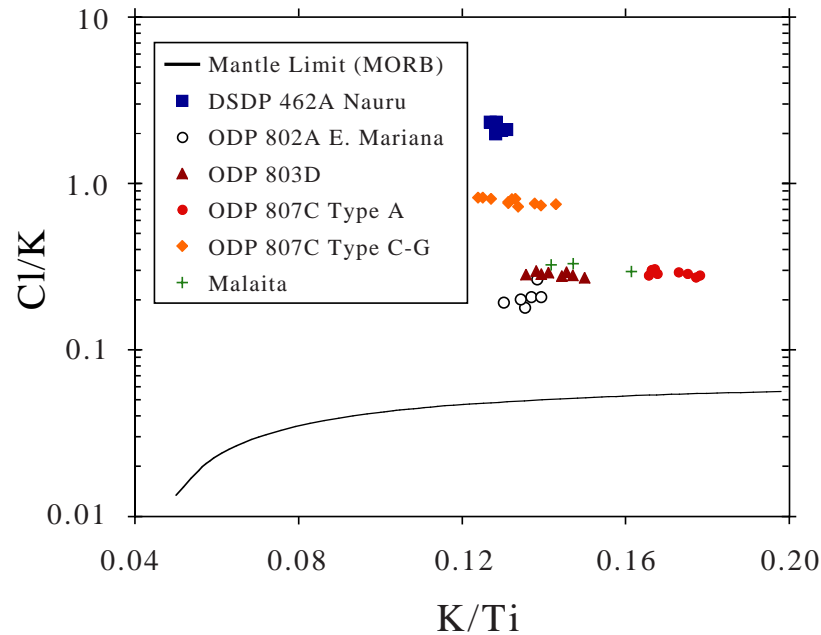
|                            | SiO <sub>2</sub> | TiO <sub>2</sub> | Al <sub>2</sub> O <sub>3</sub> | FeO          | MnO         | MgO         | CaO          | Na <sub>2</sub> O | K <sub>2</sub> O | P <sub>2</sub> O <sub>5</sub> | Cl           | H <sub>2</sub> O | CO <sub>2</sub> | Total         | Ce          | Crystallization P |            |            | Na <sub>8,0</sub> | P Eq.<br>CO <sub>2</sub> |
|----------------------------|------------------|------------------|--------------------------------|--------------|-------------|-------------|--------------|-------------------|------------------|-------------------------------|--------------|------------------|-----------------|---------------|-------------|-------------------|------------|------------|-------------------|--------------------------|
|                            |                  |                  |                                |              |             |             |              |                   |                  |                               |              |                  |                 |               |             | PD                | PY         | PWN        |                   |                          |
| <i>Nauru Basin</i>         |                  |                  |                                |              |             |             |              |                   |                  |                               |              |                  |                 |               |             |                   |            |            |                   |                          |
| 462A-47R-2, 54-55          | 50.95            | 0.91             | 14.51                          | 10.52        | 0.20        | 8.12        | 12.14        | 1.95              | 0.084            | 0.07                          | 0.197        | 0.134            | 0.0096          | 99.89         | 6.4         | 1.6               | 3.3        | 2.5        | 1.98              | 209                      |
| 462A-47R-3, 75-76          | 51.56            | 0.92             | 14.55                          | 10.57        | 0.21        | 7.98        | 12.05        | 1.95              | 0.084            | 0.06                          | 0.197        | 0.143            | 0.0095          | 100.39        | 6.4         | 1.0               | 3.0        | 2.5        | 1.94              | 207                      |
| 462A-51R-4, 28-30          | 51.80            | 1.01             | 14.15                          | 11.00        | 0.20        | 7.81        | 11.91        | 2.03              | 0.950            | 0.07                          | 0.197        | 0.152            | 0.0105          | 99.92         | 7.1         | 1.0               | 2.6        | 2.3        | 1.98              | 229                      |
| 462A-56R-1, 9-10           | 50.63            | 1.00             | 14.11                          | 10.95        | 0.19        | 7.89        | 12.09        | 2.05              | 0.095            | 0.07                          | 0.199        | 0.160            | 0.0104          | 99.55         | 6.1         | 1.1               | 2.7        | 1.9        | 2.02              | 227                      |
| 462A-69R-1, 12-13          | 50.46            | 1.08             | 13.75                          | 11.23        | 0.18        | 7.51        | 11.85        | 2.13              | 0.100            | 0.07                          | 0.198        | 0.186            | 0.0110          | 98.87         | 6.3         | 0.7               | 1.9        | 1.4        | 2.00              | 241                      |
| <b>Average 462A</b>        | <b>50.96</b>     | <b>0.98</b>      | <b>14.21</b>                   | <b>10.85</b> | <b>0.20</b> | <b>7.86</b> | <b>12.01</b> | <b>2.02</b>       | <b>0.092</b>     | <b>0.07</b>                   | <b>0.198</b> | <b>0.155</b>     | <b>0.0102</b>   | <b>99.72</b>  | <b>6.4</b>  | <b>1.1</b>        | <b>2.7</b> | <b>2.1</b> | <b>1.98</b>       | <b>223</b>               |
| <i>East Mariana Basin</i>  |                  |                  |                                |              |             |             |              |                   |                  |                               |              |                  |                 |               |             |                   |            |            |                   |                          |
| 802A-58R-2, 117-122        | 51.97            | 1.17             | 13.75                          | 11.91        | 0.18        | 7.12        | 11.21        | 1.97              | 0.116            | 0.09                          | 0.240        | 0.282            | 0.0102          | 99.89         | 7.1         | 0.2               | 2.0        | 2.8        | 1.73              | 227                      |
| 802A-58R-2, 142-149        | 52.02            | 1.15             | 13.73                          | 11.95        | 0.21        | 6.93        | 11.14        | 1.96              | 0.116            | 0.08                          | 0.024        | 0.297            | 0.0109          | 99.72         | 8.2         | 0.2               | 1.7        | 2.5        | 1.67              | 243                      |
| 802A-58R-4, 65-70          | 51.30            | 1.17             | 13.78                          | 11.92        | 0.21        | 7.10        | 11.20        | 2.00              | 0.117            | 0.08                          | 0.031        | 0.289            | 0.0107          | 99.31         | 8.3         | 0.4               | 2.3        | 2.9        | 1.76              | 238                      |
| 802A-58R-4, 67-68          | 51.37            | 1.14             | 13.91                          | 12.24        | 0.25        | 7.25        | 11.38        | 2.01              | 0.111            | 0.07                          | 0.020        | 0.289            | 0.0107          | 100.14        | 8.3         | 0.7               | 2.8        | 2.9        | 1.81              | 238                      |
| 802A-59R-1, 131-132        | 51.67            | 1.18             | 13.90                          | 12.22        | 0.25        | 7.15        | 11.35        | 1.92              | 0.114            | 0.09                          | 0.023        |                  |                 | 99.96         |             | 0.2               | 2.6        | 2.7        | 1.69              |                          |
| 802A-59R-2, 56-57          | 50.80            | 1.16             | 13.71                          | 12.07        | 0.23        | 7.15        | 11.35        | 2.04              | 1.109            | 0.07                          | 0.021        |                  |                 | 98.80         |             | 0.5               | 2.3        | 2.6        | 1.81              |                          |
| <b>Average 802A</b>        | <b>51.52</b>     | <b>1.16</b>      | <b>13.80</b>                   | <b>12.05</b> | <b>0.22</b> | <b>7.12</b> | <b>11.27</b> | <b>1.98</b>       | <b>0.110</b>     | <b>0.08</b>                   | <b>0.024</b> | <b>0.289</b>     | <b>0.0106</b>   | <b>99.64</b>  | <b>8.0</b>  | <b>0.3</b>        | <b>2.3</b> | <b>2.7</b> | <b>1.74</b>       | <b>236</b>               |
| <i>Ontong Java Plateau</i> |                  |                  |                                |              |             |             |              |                   |                  |                               |              |                  |                 |               |             |                   |            |            |                   |                          |
| 803D-69R-2, 1-2            | 50.03            | 1.25             | 14.51                          | 11.61        | 0.21        | 7.83        | 12.09        | 2.10              | 0.125            | 0.09                          | 0.037        | 0.250            | 0.0182          | 100.28        | 10.1        | 1.9               | 4.0        | 2.6        | 2.05              | 397                      |
| 803D-69R-3, 54-55          | 49.80            | 1.30             | 14.38                          | 11.69        | 0.24        | 7.83        | 12.10        | 2.11              | 0.127            | 0.09                          | 0.036        | 0.251            | 0.0184          | 100.11        | 12.3        | 1.9               | 3.6        | 2.5        | 2.06              | 401                      |
| 803D-69R-3, 110-111        | 50.08            | 1.28             | 14.33                          | 11.48        | 0.22        | 7.70        | 11.95        | 2.11              | 0.133            | 0.10                          | 0.037        | 0.274            |                 | 99.82         | 12.3        | 1.8               | 3.3        | 2.5        | 2.03              |                          |
| 803D-70R-1, 112-113        | 50.95            | 1.24             | 14.47                          | 11.58        | 0.22        | 7.75        | 11.96        | 2.17              | 0.130            | 0.07                          | 0.038        |                  |                 | 100.72        | 10.6        | 1.7               | 3.0        | 2.8        | 2.10              |                          |
| 803D-70R-2, 119-120        | 49.77            | 1.26             | 14.33                          | 11.62        | 0.21        | 7.77        | 12.25        | 2.15              | 0.127            | 0.11                          | 0.036        | 0.280            | 0.0197          | 100.06        | 10.6        | 1.7               | 3.6        | 1.8        | 2.09              | 430                      |
| 803D-70R-2, 6-7            | 50.37            | 1.21             | 14.40                          | 11.55        | 0.21        | 7.55        | 12.10        | 2.08              | 0.129            | 0.07                          | 0.036        |                  |                 | 99.84         | 10.6        | 1.0               | 2.8        | 1.7        | 1.96              |                          |
| 803D-71R-2, 10-11          | 50.17            | 1.23             | 14.38                          | 11.60        | 0.21        | 7.74        | 12.13        | 2.10              | 0.133            | 0.11                          | 0.036        | 0.284            | 0.0218          | 100.28        | 10.2        | 1.6               | 4.0        | 2.1        | 2.03              | 475                      |
| 803D-71R-3, 9-10           | 49.55            | 1.28             | 14.70                          | 11.64        | 0.22        | 7.60        | 12.28        | 2.18              | 0.130            | 0.10                          | 0.038        | 0.292            | 0.0223          | 100.17        | 10.2        | 1.5               | 3.8        | 1.9        | 2.07              | 486                      |
| <b>Average 803D</b>        | <b>50.09</b>     | <b>1.26</b>      | <b>14.44</b>                   | <b>11.60</b> | <b>0.22</b> | <b>7.72</b> | <b>12.11</b> | <b>2.13</b>       | <b>0.129</b>     | <b>0.09</b>                   | <b>0.037</b> | <b>0.272</b>     | <b>0.0201</b>   | <b>100.16</b> | <b>10.9</b> | <b>1.6</b>        | <b>3.5</b> | <b>2.2</b> | <b>2.05</b>       | <b>438</b>               |
| 807C-74R-4, 98-100         | 49.77            | 1.60             | 14.14                          | 12.21        | 0.20        | 7.43        | 11.81        | 2.40              | 0.202            | 0.11                          | 0.058        | 0.444            | 0.0052          | 100.52        | 15.0        | 2.4               | 3.0        | 2.5        | 2.25              | 130                      |
| 807C-74R-4, 98-100         | 49.88            | 1.60             | 14.06                          | 12.00        | 0.21        | 7.03        | 11.53        | 2.35              | 0.202            | 0.11                          | 0.058        | 0.444            | 0.0048          | 99.69         | 15.0        | 1.5               | 2.3        | 2.3        | 2.09              | 121                      |
| 807C-75R-2, 73-75          | 50.10            | 1.62             | 14.12                          | 12.10        | 0.24        | 7.06        | 11.70        | 2.36              | 0.202            | 0.14                          | 0.059        | 0.492            | 0.0042          | 100.34        | 14.7        | 1.1               | 2.4        | 1.9        | 2.11              | 112                      |
| 807C-76R-1, 57-58          | 50.23            | 1.61             | 14.40                          | 11.94        | 0.31        | 7.12        | 11.75        | 2.41              | 0.193            | 0.11                          | 0.058        | 0.400            | 0.0061          | 100.54        | 14.7        | 1.5               | 2.6        | 2.2        | 2.17              | 146                      |
| 807C-77R-2, 108-110        | 49.78            | 1.61             | 14.05                          | 12.02        | 0.21        | 7.15        | 11.70        | 2.34              | 0.207            | 0.10                          | 0.058        | 0.385            | 0.0049          | 99.75         | 15.2        | 1.4               | 2.5        | 2.2        | 2.11              | 119                      |
| 807C-77R-36-37             | 50.13            | 1.64             | 14.33                          | 12.16        | 0.24        | 7.13        | 11.64        | 2.36              | 0.196            | 0.13                          | 0.055        | 0.401            | 0.0055          | 100.42        | 14.4        | 1.6               | 2.8        | 2.6        | 2.13              | 133                      |
| 807C-77R-2, 107-108        | 49.82            | 1.60             | 14.16                          | 12.03        | 0.25        | 7.06        | 11.83        | 2.42              | 0.193            | 0.12                          | 0.059        | 0.399            | 0.0057          | 99.95         | 14.4        | 1.3               | 2.2        | 1.5        | 2.17              | 137                      |
| 807C-78R-1, 33-34          | 49.34            | 1.63             | 14.10                          | 12.10        | 0.30        | 7.02        | 11.72        | 2.47              | 0.196            | 0.12                          | 0.059        | 0.388            | 0.0049          | 99.45         | 15.2        | 1.6               | 2.5        | 1.8        | 2.21              | 119                      |
| 807C-79R-4, 21-23          | 49.42            | 1.61             | 13.78                          | 12.05        | 0.17        | 7.27        | 11.74        | 2.35              | 0.206            | 0.11                          | 0.056        | 0.372            | 0.0076          | 99.28         | 15.4        | 1.7               | 2.4        | 1.8        | 2.15              | 177                      |
| <b>Average 807C A</b>      | <b>49.83</b>     | <b>1.69</b>      | <b>14.13</b>                   | <b>12.07</b> | <b>0.24</b> | <b>7.14</b> | <b>11.71</b> | <b>2.38</b>       | <b>0.200</b>     | <b>0.12</b>                   | <b>0.058</b> | <b>0.414</b>     | <b>0.0054</b>   | <b>99.99</b>  | <b>14.9</b> | <b>1.6</b>        | <b>2.5</b> | <b>2.1</b> | <b>2.15</b>       | <b>132</b>               |



Table 1 (continued). Chemistry and Crystallization Pressures of Glasses From Nauru Basin, Ontong Java Plateau, and East Mariana

|                         | SiO <sub>2</sub> | TiO <sub>2</sub> | Al <sub>2</sub> O <sub>3</sub> | FeO          | MnO         | MgO         | CaO          | Na <sub>2</sub> O | K <sub>2</sub> O | P <sub>2</sub> O <sub>5</sub> | Cl           | H <sub>2</sub> O | CO <sub>2</sub> | Total        | Ce         | Crystallization P |            |            | Na <sub>8,0</sub> | P Eq.<br>CO <sub>2</sub> |
|-------------------------|------------------|------------------|--------------------------------|--------------|-------------|-------------|--------------|-------------------|------------------|-------------------------------|--------------|------------------|-----------------|--------------|------------|-------------------|------------|------------|-------------------|--------------------------|
|                         |                  |                  |                                |              |             |             |              |                   |                  |                               |              |                  |                 |              |            | PD                | PY         | PWN        |                   |                          |
| 807C-80R-4, 81-81       | 50.87            | 1.12             | 13.95                          | 12.10        | 0.20        | 7.18        | 11.58        | 2.15              | 0.108            | 0.10                          | 0.087        | 0.253            | 0.0149          | 99.72        | 9.4        | 0.6               | 2.3        | 2.2        | 1.93              | 327                      |
| 807C-81R-1, 135-137     | 49.73            | 1.16             | 13.93                          | 12.07        | 0.21        | 7.60        | 11.86        | 2.19              | 0.110            | 0.15                          | 0.085        | 0.233            | 0.0150          | 99.46        | 9.4        | 1.8               | 3.5        | 2.4        | 2.08              | 328                      |
| 807C-82R-1, 31-32       | 50.95            | 1.14             | 13.95                          | 12.00        | 0.20        | 7.29        | 11.65        | 2.13              | 0.111            | 0.07                          |              | 0.223            | 0.0129          | 99.73        | 9.6        | 0.7               | 2.3        | 2.2        | 1.94              | 283                      |
| 807C-82R-1, 1-2         | 50.82            | 1.13             | 13.96                          | 11.98        | 0.25        | 7.31        | 11.79        | 2.22              | 0.110            | 0.07                          |              | 0.262            | 0.0153          | 99.92        | 9.4        | 0.7               | 2.2        | 1.8        | 2.03              | 335                      |
| 807C-82R-4, 36-37       | 49.86            | 1.16             | 13.80                          | 11.98        | 0.27        | 7.28        | 11.75        | 2.22              | 0.111            | 0.06                          | 0.089        | 0.239            | 0.0152          | 98.83        | 9.4        | 1.0               | 2.4        | 1.7        | 2.03              | 332                      |
| 807C-82R-5, 11-12       | 50.71            | 1.17             | 13.95                          | 11.92        | 0.24        | 7.26        | 11.72        | 2.24              | 0.106            | 0.06                          | 0.087        | 0.258            | 0.0164          | 99.74        | 9.4        | 0.7               | 2.1        | 1.9        | 2.04              | 359                      |
| 807C-82R-6, 120-121     | 50.55            | 1.16             | 13.85                          | 12.04        | 0.20        | 7.39        | 11.63        | 2.18              | 0.110            | 0.07                          | 0.084        | 0.250            | 0.0166          | 99.53        | 9.4        | 1.1               | 2.5        | 2.4        | 2.02              | 363                      |
| 807C-85R-7, 131-132     | 50.93            | 1.14             | 14.00                          | 12.07        | 0.29        | 7.29        | 11.82        | 2.14              | 0.118            | 0.06                          | 0.088        |                  |                 | 99.95        |            | 0.4               | 2.2        | 1.7        | 1.95              |                          |
| 807C-86R-2, 2-3         | 50.08            | 1.13             | 13.97                          | 11.88        | 0.22        | 7.34        | 11.85        | 2.14              | 0.104            | 0.08                          | 0.084        | 0.241            | 0.0165          | 99.13        |            | 0.8               | 2.5        | 1.6        | 1.96              | 360                      |
| 807C-86R-2, 136-137     | 50.73            | 1.14             | 13.81                          | 11.80        | 0.24        | 7.29        | 11.74        | 2.10              | 0.102            | 0.08                          | 0.084        | 0.242            | 0.0163          | 99.37        |            | 0.3               | 2.0        | 1.6        | 1.91              | 356                      |
| 807C-90R-3, 60-63       | 50.13            | 1.09             | 13.91                          | 11.85        | 0.23        | 7.76        | 11.94        | 2.11              | 0.110            | 0.09                          | 0.081        | 0.223            | 0.0161          | 99.66        | 8.9        | 1.5               | 3.3        | 2.3        | 2.05              | 351                      |
| 807C-90R-2, 118-119     | 50.88            | 1.14             | 13.95                          | 11.76        | 0.24        | 7.34        | 11.61        | 2.12              | 0.110            | 0.07                          | 0.080        | 0.252            | 0.0171          | 99.57        | 9.1        | 0.8               | 2.4        | 2.4        | 1.94              | 373                      |
| 807C-92R-2, 113-117     | 51.06            | 1.09             | 14.02                          | 11.65        | 0.23        | 7.27        | 11.89        | 2.05              | 0.108            | 0.15                          | 0.082        | 0.225            | 0.0174          | 99.96        | 8.5        | 0.0               | 1.9        | 1.2        | 1.85              | 379                      |
| <b>Average 807C C-G</b> | <b>50.56</b>     | <b>1.14</b>      | <b>13.93</b>                   | <b>11.93</b> | <b>0.23</b> | <b>7.35</b> | <b>11.76</b> | <b>2.15</b>       | <b>0.109</b>     | <b>0.09</b>                   | <b>0.085</b> | <b>0.242</b>     | <b>0.0158</b>   | <b>99.58</b> | <b>9.5</b> | <b>0.8</b>        | <b>2.4</b> | <b>2.0</b> | <b>1.98</b>       | <b>345</b>               |
| <i>Malaita</i>          |                  |                  |                                |              |             |             |              |                   |                  |                               |              |                  |                 |              |            |                   |            |            |                   |                          |
| Malaita 1               | 50.58            | 1.63             | 13.57                          | 12.89        | 0.23        | 6.59        | 11.01        | 1.66              | 0.190            | 0.11                          | 0.056        | 1.250            |                 | 99.91        | 15.7       | 0.1               |            | 2.4        | 1.28              |                          |
| Malaita 2               | 50.13            | 1.60             | 13.53                          | 12.77        | 0.22        | 6.39        | 11.04        | 1.48              | 0.170            | 0.11                          | 0.056        | 0.710            |                 | 98.35        | 16.0       | -0.5              |            |            | 1.05              |                          |
| Malaita 3               | 50.40            | 1.66             | 13.62                          | 13.05        | 0.21        | 6.48        | 11.16        | 2.01              | 0.170            | 0.11                          | 0.055        | 0.770            |                 | 99.85        | 16.0       | -0.4              |            | 1.9        | 1.60              |                          |
| <b>Average Malaita</b>  | <b>50.37</b>     | <b>1.63</b>      | <b>13.57</b>                   | <b>12.90</b> | <b>0.22</b> | <b>6.49</b> | <b>11.07</b> | <b>1.72</b>       | <b>0.180</b>     | <b>0.11</b>                   | <b>0.060</b> | <b>0.910</b>     |                 | <b>99.37</b> |            | <b>-0.3</b>       |            | <b>2.1</b> | <b>n.d.</b>       |                          |
| Standard JDF-D2         | 50.59            | 1.89             | 13.78                          | 12.14        | 0.26        | 6.75        | 10.66        | 2.70              | 0.291            | 0.23                          | 0.030        | 0.344            | 0.0268          | 99.60        |            |                   |            |            |                   |                          |
| 1 σ (std. dev.)         | 0.30             | 0.03             | 0.11                           | 0.10         | 0.02        | 0.15        | 0.09         | 0.04              | 0.009            |                               | 0.001        | 0.020            | 0.0020          |              |            |                   |            |            |                   |                          |

All oxides and volatiles are reported in weight percent except Ce, in ppm. Na<sub>8,0</sub> is calculated using equation by *Klein and Langmuir* [1987] and slope derived from Kolbeinsey lavas: Na/Mg equals 0.27. Averages are provided because most samples within a group are within analytical uncertainty, except 462A. Ce (in ppm) is taken from nearest analysis in core as reported by *Mahoney et al.* [1993a]. Crystallization pressures are in kilobars and were obtained using three different models: PY, *Yang et al.* [1996]; PD, *Danyushevsky et al.* [1996]; PW, *Weaver and Langmuir* [1990]. P equil CO<sub>2</sub> is the pressure (in bars) at which liquid would be saturated with a CO<sub>2</sub> plus H<sub>2</sub>O volatile phase. It should correspond to the maximum eruption pressure [*Dixon et al.*, 1995].



**Figure 3.** *Cl/K versus K/Ti. Note the logarithmic scale for Cl/K. K/Ti is an indicator of mantle source enrichment:  $K/Ti < 0.13$  in N-MORB and  $K/Ti > 0.22$  in E-MORB. Note the limited range of K/Ti. The mantle trend is derived from N-MORB through E-MORB ( $K/Ti = 0.020.7$ ) that have erupted on ridges with low magma flux. Mid-ocean ridges with high magma flux often have Cl/K above this trend, up to 0.7. The higher values are presumed to be related to assimilation of seawater-derived components [Michael and Cornell, 1998].*

in composition. However, the long distances between sites and differences in trace element and isotopic ratios between sites preclude the glasses from actually being related to each other. (Crystallization models are discussed in section 6.1.2). There are small but significant differences in K/Ti (Figure 3), an indicator of source composition that should be nearly unaffected by fractionation. Hole 462A and Hole 807C types CG have the lowest K/Ti, while type A in Hole 807C has the highest ratio and Holes 802A and 803D are intermediate. There are also deviations from simple trends that show up as scatter in diagrams of MgO versus oxides. For example, Hole 807 type A has higher  $K_2O$ ,  $TiO_2$  (not shown),  $Na_2O$ , and K/Ti than the trend for other glasses. Glass from Hole 802A has lower  $Na_2O$  and CaO and higher  $SiO_2$  at a given MgO than the other glasses. The relation of these differences to variations in source composition and extent of melting is discussed in section 6.3.

## 5.2. Chlorine

[15] Cl contents range widely from 200 to 1990 ppm (Table 1). These values were obtained on clear, fresh

glass fragments and are constant within each glass layer (and even between adjacent glass layers), so they represent magmatic concentrations that were not influenced by post-eruptive alteration. The Cl concentrations are high compared to most MORB (20400 ppm) and are remarkably constant within a core, even for the different chemical types of 462A. The altered glasses from Malaita have similar Cl and Cl/K as the 807 type A glasses, suggesting that alteration did not affect Cl or K significantly.

[16] Cl/K is unaffected by partial melting and simple fractional crystallization, and has been defined for mantle sources (Figure 3) [Michael and Cornell, 1998]. Cl/K above these values ( $>0.07$ ) has been attributed to assimilation of hydrothermally altered material, possibly brine [Michael and Schilling, 1989]. Cl/K is very high for all glasses analyzed, compared to MORB and ocean island basalts (OIB) that have not been affected by assimilation (Figure 3). Cl/K is not correlated with MgO for the OJP/EMB/NB glasses as a group, unlike MORB from fast-spreading ridges. Cl/K ratios are actually higher at a given MgO than those for most MORB. Cl and Cl/K are the highest ever measured in



basalts for all three chemical types from Hole 462A. It is surprising that all three chemical types share this trait, even though their major element chemistry varies slightly.

### 5.3. CO<sub>2</sub>

[17] Dissolved CO<sub>2</sub> is present completely as CO<sub>3</sub><sup>2-</sup>. No molecular CO<sub>2</sub> was detected. CO<sub>2</sub> concentrations in Hole 807C are 54 ± 10 ppm in type A and 158 ± 20 ppm in types CG basalts. Concentrations are 103 ± 7 ppm in glasses from Hole 802A and 462A. Glasses from Hole 803D had 201 ± 19 ppm CO<sub>2</sub>. Analytical errors are significant (20%) because concentrations are low. Standard deviations for multiple analyses within the same flow and within the same chemical type are smaller than the analytical error, suggesting that the measured abundances are reliable magmatic values and have not been strongly influenced by alteration or by the formation of microlites.

### 5.4. H<sub>2</sub>O

[18] Dissolved H<sub>2</sub>O is present almost entirely as OH<sup>-</sup>, the hydroxyl ion, and varies from 0.13 in NB glasses to

0.5 in OJP glasses (Table 1). Areas of alteration were avoided during analysis. Concentrations are fairly homogeneous within flows and within chemical types, except for 807C, type A. Moreover, the very low (or zero) values of H<sub>2</sub>O<sub>M</sub>/(H<sub>2</sub>O<sub>M</sub>+OH<sup>-</sup>) are consistent with H<sub>2</sub>O speciation expected for magmas [Dixon *et al.*, 1988; Stolper, 1982], and not altered glass. Thus H<sub>2</sub>O contents represent magmatic values, unaffected by surficial alteration or uptake during eruption. The measureable CO<sub>2</sub> contents, the proposed eruption depths, and the lack of vesicles in the lavas all suggest that H<sub>2</sub>O did not degas significantly during eruption. The assimilation of altered material (see section 6.1.3) probably did not significantly affect H<sub>2</sub>O contents based on similar studies of MORB [Michael and Cornell, 1998; Michael and Schilling, 1989] and on the fact that the glasses with the highest Cl have the lowest H<sub>2</sub>O. Thus the H<sub>2</sub>O contents represent primary magmatic values that can be used to describe the glasses' mantle source. H<sub>2</sub>O contents are broadly similar to MORB and are lower than arc-related magmas.

[19] For most MORB, H<sub>2</sub>O/Ce ratios are constant from N-MORB to E-MORB, and fall mostly in the range of 150-250, while MORB around Iceland and the north-

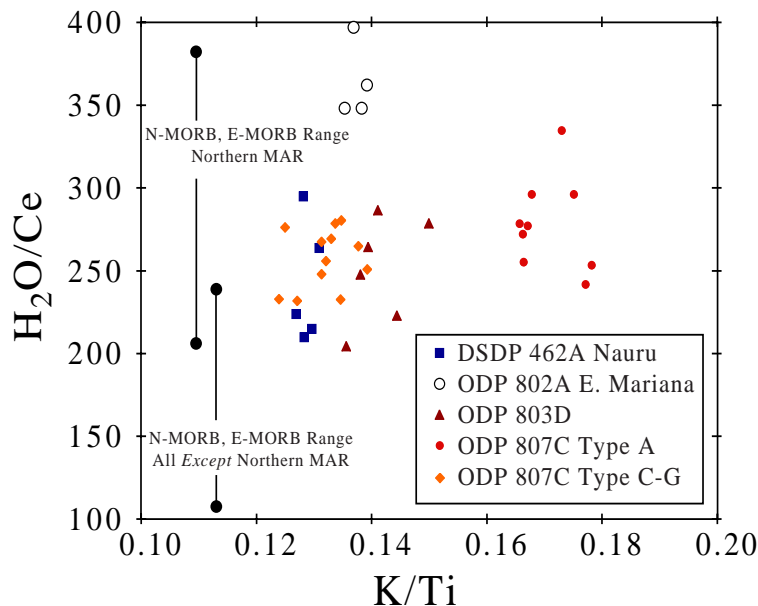


**Figure 4.** H<sub>2</sub>O/Ce versus K/Ti. H<sub>2</sub>O/Ce is roughly constant from N-MORB to E-MORB but varies regionally. In particular, the Mid-Atlantic Ridge north of 30°N has higher H<sub>2</sub>O/Ce than the rest of the ridge system [Michael, 1995]. H<sub>2</sub>O/Ce > 500 in glasses associated with island arcs [Stolper and Newman, 1994]. Note that the Cretaceous glasses have H<sub>2</sub>O/Ce ratios that exceed those of most MORB and are similar to the northern MAR. Glasses from Malaita are not shown because they are affected by alteration. Note the limited range of K/Ti compared to MORB.

ernmost MAR are higher: from 220 to 380 [Michael, 1995] (Figure 4).  $H_2O/REE$  for arc related magmas are much higher [Stolper and Newman, 1994], typically  $>500$ .  $H_2O/Ce$  ratios in OJP, NB, and EMB glasses are high compared to most MORB but not as high as arc-related glasses and are similar to the anomalously high northern MAR glasses [Michael, 1995] (Figure 4).

## 6. Discussion

### 6.1. Magma Chamber Characteristic

#### 6.1.1. Magma homogeneity

[20] Within each chemical type (up to 100 m thick, with  $>40$  cooling units) the glasses show considerably less geochemical variability than similar drilled sections of MORB glasses [Fisk *et al.*, 1996] or even continental flood basalts [Hooper, 1997]. The fact that many different cooling units have nearly identical chemistry suggests that each chemical type represents a single eruptive episode that was made up of many lava flows or surges, or lobes, in the terminology of Self *et al.* [1997]. In Hole 807C,  $\sim 7$  cm of sediment separates basalt layers with identical chemistry: units 4C and 4E [Kroenke *et al.*, 1991], suggesting some time elapsed during this eruptive episode. If this does represent a time interval, such homogeneity would require a very large, well-mixed, and/or strongly buffered magma chamber. It also suggests that the magmas did not travel very far from this reservoir. It is impossible to estimate the areal extent or volumes of any of the basalt chemical types to compare with terrestrial flood basalts.

#### 6.1.2. Crystallization depth.

[21] By analogy with chemically similar MORB and based on petrography of relict or altered phases [Kroenke *et al.*, 1991] these fractionated lavas must have evolved by crystallization of a three phase assemblage consisting of olivine (OL), plagioclase (PL), and clinopyroxene (CPX). By assuming that the glasses are in equilibrium with these three phases, depths of crystallization can be calculated for each glass (Table 1) using three different major element models that describe MORB crystallization [Danyushevsky *et al.*, 1996; Weaver and Langmuir, 1990; Yang *et al.*, 1996]. The methods rely on the fact that the  $dT/dP$  of CPX saturation is significantly greater than that of OL or PL, so as a magma ascends, CPX becomes relatively more undersaturated. A calculated depth represents a minimum for the initiation of crystallization because a

magma may have started crystallizing deeper, and then continually crystallized and equilibrated to some extent as it ascended. The depth represents a maximum for the completion of crystallization, because a magma may have been crystallizing OL+PL+CPX at depth, and then ascended to shallower levels without reattaining saturation (equilibrium) with OL+PL+CPX. The three different methods and associated errors are discussed fully by Michael and Cornell [1998]. Calculated crystallization pressures vary depending on the model used, but in each case they are in the low end of the range of pressures calculated for MORB [Michael and Cornell, 1998]. The pressures are similar to those from fast-spreading ridges like EPR or robust slow-spreading ridges like Kolbeinsey Ridge north of Iceland. Surprisingly, there are no significant differences in crystallization pressures between glasses from OJP and NB and EMB. Calculated crystallization pressures (Table 1) require that a significant amount of crystallization took place at shallow levels. Fast seismic velocities in the lower crustal levels of OJP have been attributed to olivine-rich cumulates that formed by crystallization at high pressure [Farnetani *et al.*, 1996]. Deep and shallow crystallization are not mutually exclusive. Indeed, Farnetani *et al.* [1996] preferred a two-stage model in which picritic magmas first crystallized at MOHO levels and then at shallower levels.

[22] The modeling and discussion below help constrain (1) the amounts of total crystallization, (2) the amount of shallow crystallization that is required to account for the glasses' current compositions, and (3) the amount of OJP's thickness that may be attributed to cumulates formed by crystallization of magmas at deeper crustal depths.

[23] Similar to earlier models [Farnetani *et al.*, 1996], major element compositional evolution was modeled as a two-stage process, with the first stage at 8 kbar and the second stage at 2 kbar. The primary magma composition is unknown, so as a plausible starting point, a picrite magma with  $\sim 16\%$  MgO (similar to the composition used previously [Farnetani *et al.*, 1996]) is used. Uncertainty in the primary magma composition leads to uncertainty in the amounts of crystallization and probably leads to some misfit between the models and data (Figure 2). By using a similar composition as the earlier studies [Neal *et al.*, 1997; Farnetani *et al.*, 1996] the results can be compared. The model used here [Weaver and Langmuir, 1990] was designed for MORB, so it should be applicable to these tholeiitic compositions. It uses experimentally constrained

distribution coefficients and phase proportions to calculate a LLD, so it should be more accurate than models using arbitrary or observed phase proportions [Neal *et al.*, 1997]. If all crystallization occurred at 8 kbar, the resulting derivative liquids would have CaO and SiO<sub>2</sub> that are much lower and FeO that is much higher than the observed compositions (Figure 2). If all crystallization occurs at 2 kbar, the derivative liquids match the observed compositions much more closely (Figure 2). These results are consistent with the calculated crystallization pressures in Table 1. Total crystallization to attain the fractionated compositions (e.g., 7.2% MgO) from the picrite ranges from ~65% at 8 kbar to ~55% at 2 kbar. Model simulations with varying amounts of early crystallization at 8 kbar show that the observed compositions and trends can be reproduced with up to 3035% crystallization at 8 kbar, followed by the remainder of crystallization (~2530%) at 2 kbar. Greater amounts of crystallization at 8 kbar, such as 46% crystallization at 8 kbar in Figure 2, are unable to reproduce the observed compositions or trends. Thus a significant amount of shallow crystallization is required. A maximum of ~1/3 of the initial melt could have crystallized at 25-km depth. This raises the possibility that some of the plateau was built up by the vertical stacking of successive shallow eruptive systems. In this case the high seismic velocities at the base of OJP might be partly due to the metamorphic grade of the rocks [Gladzenko *et al.*, 1997].

### 6.1.3. Cl and assimilation.

[24] Very high Cl/K in every flow type suggests that ascending magmas encountered and assimilated rocks that had been affected by hydrothermal alteration [Michael and Cornell, 1998]. This, in turn, suggests that hydrothermal activity was widespread on OJP, EMB, and NB. High Cl in MORB is associated with low crystallization pressures and often with a shallow axial magma chamber [Michael and Cornell, 1998]. The necessary conditions are probably modulated by magma flux so are favored by a fast-spreading rate but are also present on slow-spreading ridges formed by large extents of melting [Michael and Cornell, 1998]. Very high Cl in OJP lavas shows that extremely vigorous shallow magmatic and hydrothermal systems may have been formed by the voluminous magmas that constructed the plateau. The lack of correlation of Cl/K with Mg# for OJP, NB, and EMB is unlike the correlation observed along the southern EPR and suggests that crustal alteration might have been heterogeneous

on a timescale and/or distance scale that was larger than that of the magma chambers.

[25] The constant high Cl (1975 ± 8 ppm) in the three compositional types analyzed from Hole 462A is a curious feature that seems to be inconsistent with assimilation, which should be a more random process. For the three sample types analyzed from Hole 462A, TiO<sub>2</sub>, FeO, Na<sub>2</sub>O, K<sub>2</sub>O, and H<sub>2</sub>O increase while MgO and Al<sub>2</sub>O<sub>3</sub> decrease. These trends are consistent with 510% fractional crystallization and suggest that the three types may be variably differentiated liquids from the same magmatic system. The only problem with this explanation is that Cl should also increase, from 1975 to ~2100 ppm. It is not likely that Cl saturation accounts for the constant Cl, since Cl saturation would be >2% in a H<sub>2</sub>O-poor basalt melt like this [Webster *et al.*, 1999]. An alternative explanation for high Cl/K in Hole 462A (and the other glasses as well) is that the mantle source of the basalts is enriched in Cl, possibly from recycled subducted altered material [Jambon *et al.*, 1995]. However, Cl/K in OJP and related glasses is not correlated with any other features that are indicative of recycling. Pb and Sr isotopic ratios and trace element ratios (e.g., Ba/Ta) in glasses from Hole 462A are within errors of the Hole 807A types CG ([Mahoney *et al.*, 1993a], and references therein). In summary, an assimilation origin is favored for the high Cl/K in all of these glasses, but the extreme and constant values in Hole 462A are difficult to explain.

### 6.2. Depths of Eruption

[26] Maximum depths of eruption are calculated for these Cretaceous glasses in Figure 5. by using experimentally determined saturation curves [Dixon *et al.*, 1995] and by assuming that glasses are saturated or oversaturated with a combined CO<sub>2</sub> + H<sub>2</sub>O volatile phase at their depth of eruption. This method relies on the strong pressure dependence of CO<sub>2</sub> solubility in magmas, and the fact that modern submarine basalt glasses are rarely undersaturated with respect to CO<sub>2</sub> [Dixon *et al.*, 1988] unless they are associated with subaerial or shallow submarine volcanoes [Dixon *et al.*, 1991]. Deeply erupted tholeiitic glasses typically lose significant amounts of CO<sub>2</sub> but very little H<sub>2</sub>O during ascent from the mantle because of the way these gases partition between melt and vapor [Dixon *et al.*, 1995] and because initial H<sub>2</sub>O concentrations are low. The calculated depths are maxima because some glasses are oversaturated as they did not have time to degas be-

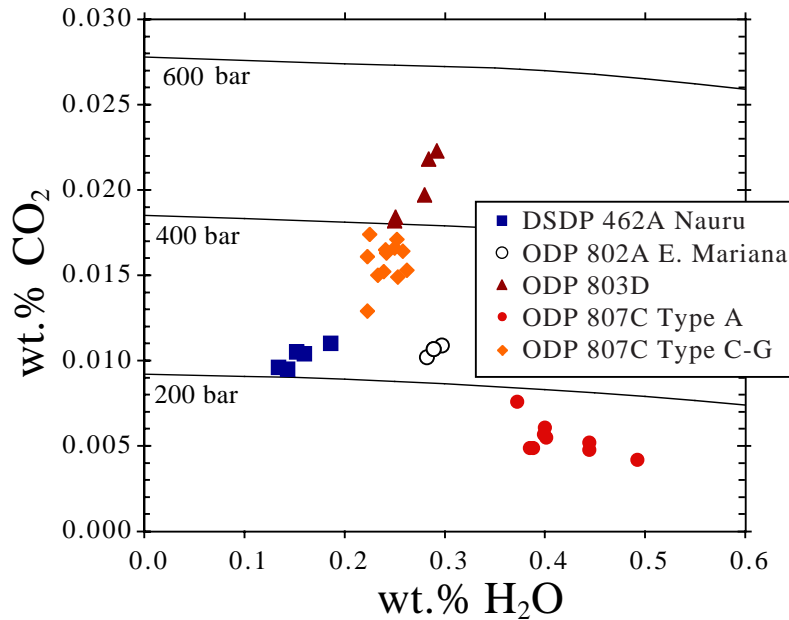


**Figure 5.**  $H_2O$  versus  $CO_2$ , showing contours of pressure at which various combinations of  $H_2O$  and  $CO_2$  will be saturated. The curves are excerpted from Dixon et al. [1995]. For seawater, depth in meters is 10 pressure in bars. Eruption pressures presented in Tables 1 and 2 are estimated from this diagram and the equations on which it is based. If glasses are oversaturated, their eruption depth will be too high.

fore cooling, and therefore record a pressure that is too high.

[27] The maximum depth of eruption (Tables 1 and 2) calculated for Hole 807C type A glasses, even accounting for the analytical uncertainty in  $CO_2$  is  $1320 \pm 250$  m, which is shallower than the lower bathyal depth range (2000-2800 m; [Sliter and Leckie, 1993]) that was estimated based on planktonic foraminifers in overlying sediments. The greater eruption depths are based on estimations of the Cretaceous carbonate compensation depth (CCD) and perturbations of the CCD near a submarine plateau. Eruption depths below the CCD were proposed for the Malaita sites by Neal et al. [1997] and Saunders et al. [1994] on the basis of the lack of calcareous sediments. It is remotely possible that  $CO_2$  was undersaturated during eruption, but this is rare for MORB [Dixon et al., 1988; P.J. Michael, unpublished data, 1999] and is highly unlikely here. It is more likely that depth estimates for Hole 807C that are based on sediments are too great. The depth calculated using  $CO_2$  in the glass is nearly within error of the shallowest depth estimated for this site (1800 m) by Ito and Clift [1998].

[28] One way to account for the discrepancy between paleoeruption depths calculated from  $CO_2$  in 807C type

A glasses and the estimates based on sediments would be to suppose that the lavas were erupted from a shallower edifice and then flowed downslope for hundreds of km to their current location. The most likely source is ~1000 m shallower than Site 807C and 450 km distant. Such long flow distances may be possible for the 28-m-thick flow of unit F but are much less likely (not impossible [S. Self, personal communication, 1999]) for the many flows that are <2 m thick in units A and CG [Mahoney et al., 1993a; P. Hooper, personal communication, 1998]. The fact that types CG lavas give much greater eruption depths (3420 m) than type A is consistent with the type CG glasses having been oversaturated with  $CO_2$  upon emplacement and cooling. If they were in fact oversaturated, they could not have traveled far from their eruptive source; otherwise, they would have degassed.

[29] The 1320-m eruption depth of 807C type A glasses falls within the broad limits of the present-day  $Na_{8,0}$  versus depth curve for hotspot-influenced MORs (Figure 6) [Langmuir et al., 1992], which is permissive evidence for eruption at or near a ridge. The greater depths estimated from sediments (2000-2800 m) also fall inside this array but is considerably deeper than the best analog for a ridge above a large plume: Iceland [Cof-



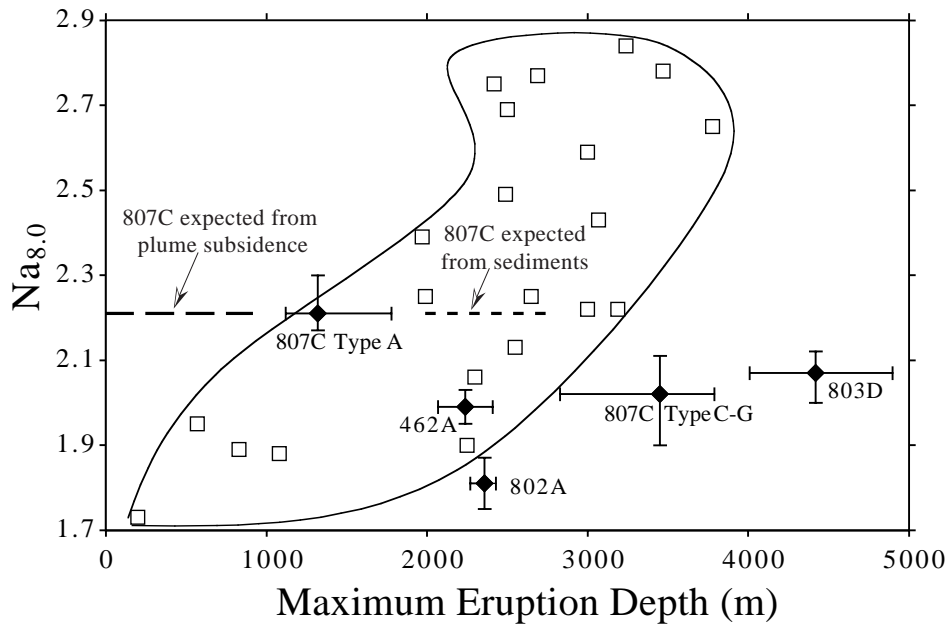


**Figure 6.**  $Na_{8.0}$  versus calculated maximum eruption chemical type corresponds to average  $Na_{8.0}$  as reported in Table 1 and average eruption depth calculated from  $CO_2$  and  $H_2O$  content as derived in Figure 5 and reported in Table 2. For each point, the horizontal bars show the range of  $CO_2$  equilibration pressures and the vertical bars show the range of  $Na_{8.0}$  for all of the samples of a particular group. The open squares and the field enclosing them denote the averages of hotspot-influenced ridges globally [Langmuir et al., 1992]. The short-dash line is the depth range estimated from sediments for Site 807C [Sliter and Leckie, 1993]. The long-dash line is the depth range (900/1000 m above sea level) that would be expected for Site 807C at 122 Ma, if it is assumed that the site subsided to its present depth after being over a plume at 122 Ma [Ito and Clift, 1998]. Notice the depth estimate from ( $H_2O + CO_2$ ) is much closer to this estimate.

fin and Gahagan, 1995]. The shallower depth strengthens arguments in favor of the formation of OJP at or near a MOR.

[30] Lavas of Hole 803D give maximum eruption depths of 4420 m, which is deeper than the present reconstructed basement depth. It is likely that the glasses are oversaturated with  $CO_2$ , and therefore do not constrain the paleoeruption depth. It is unlikely that this site has become shallower in the past 90 Myr, as it is distant from the tectonically uplifted southern part of the plateau. The oversaturation suggests that the flows did not erupt far from their present position.

[31] Maximum paleoeruption depths calculated for basin Sites 462A and 802A are 2200 and 2400 m, respectively. These depths are considerably shallower than expected for eruption of basalt onto seafloor that was perhaps already 3570 Myr old. (Extrapolation of magnetic anomalies [Nakanishi et al., 1992] in EMB and NB suggests an age of 145/170 Ma. Basalt ages from Hole 802A and 462A are 110/115 Ma [Castillo et al.,

1994]. The shallower eruption depths suggest that both basins were affected by a hotspot swell from OJP. In a plot of  $Na_{8.0}$  versus depth (Figure 5) the basin lavas fall at the deep end of the range of hotspot-influenced mid-ocean ridges. However, OJP stands 23 km above the surrounding seafloor, so it would be difficult to have both OJP and EMB and NB conform to the  $Na_{8.0}$  versus depth relationship, unless they have followed very different subsidence histories [Ito and Clift, 1998].

#### 6.2.1. Implications for plateau subsidence.

[32] Because our calculated eruption depths are maxima, our calculated subsidence amounts are minima. OJP's subsidence was calculated previously [Ito and Clift, 1998] by subtracting estimates of eruption depth from calculated basement depths in the absence of sediments (reconstructed basement depths). The amounts of subsidence were not sufficient to account for the thermal subsidence expected after passage of the lithosphere over a mild ( $T = 150^\circ C$ ) or high-





**Table 2. Sample Site and Core Characteristics**

| Hole  | DSDP | ODP  | ODP  | ODP  | ODP 807C |
|---|------|------|------|------|----------|
|   | 462A | 802A | 803D | 807C | (C-G)    |
| Present seafloor depth                      | 5187 | 5968 | 3412 | 2806 | 2806     |
| Basement depth, mbsf                        | 994  | 509  | 631  | 1380 | 1380     |
| Basalt drilled, m                           | 215  | 51   | 26   | 44   | 105      |
| Basalt recovered, m                         | 155  | 15.3 | 9.6  | 22   | 65       |
| Percent basalt recovered                    | 54   | 30   | 38   | 50   | 62       |
| Number of cooling units                     | 56   | 17   | 25   | 29   | 38       |
| Number of chemical types                    | 3+2  | 1    | 1    | 1    | 1        |
| Thickest flow, m                            | 30   | 3.2  | 1.3  | 2    | 28       |
| Average flow thickness, m                   | 3    | 3    | 1    | 1.5  | 2.1      |
| Na <sub>40</sub>                            | 1.99 | 1.81 | 2.07 | 2.21 | 2.02     |
| Max. eruption depth (from CO <sub>2</sub> ) | 2240 | 2360 | 4420 | 1320 | 3450     |
| Approx. reconstructed basement              | 5515 | 6136 | 3620 | 3261 | 3261     |
| Minimum calculated subsidence (n)           | 3275 | 3776 | -800 | 1941 | -189     |
| Subsidence expected from cooling (1)        | 2400 | 2400 | 1500 | 2400 | 2400     |
| Subsidence expected from cooling (2)        | 4400 | 4400 | 2500 | 4200 | 4200     |

Separate columns are provided for 807C chemical types A and C-G. Percent basalt recovered is meters of basement drilled/meters of basalt recovered; number of cooling units: estimated subjectively from DSDP volumes 89 and ODP volumes 129 130; number of chemical types is number of different glass types within analytical uncertainty of major element chemistry plus other types from parts of core with no glass (462A); thickest flow is the widest interval of basalt without a cooling unit break; average flow thickness is meters of basalt drilled/#cooling units (does not include 28-m-thick flow for 807C C-G); approximate reconstructed basement depths are from *Ito and Clift* [1998] directly (803D and 807C), or by using their method (462A and 802A); minimum calculated subsidence is the approximate reconstructed basement depth-maximum eruption depth; subsidence expected from cooling is based on the cooling models of *Ito and Clift* [1998], and a (1) 150°C or (2)350°C plume that affected the site at 110-120 Ma (90 Ma for 803D).

temperature ( $T = 350^\circ$ ) plume at 122 Ma. It was proposed that OJP had not subsided as much as expected because it had formed over a long time interval, perhaps by repeated episodes of magmatism and underplating after the 122 Ma event [*Ito and Clift*, 1998]. Our shallower eruption estimate for 807C allows greater subsidence of OJP than *Ito and Clift* [1998]. Using their reconstructed basement depth (3300 m) and our 1320-m eruption depth estimate, subsidence is 1980 m for Hole 807C, which is nearly enough to account for continuous cooling of lithosphere that was influenced by a mild plume at 122 Ma (~2500 m) [*Ito and Clift*, 1998]. Greater subsidence (~ 4300 m) would be expected for a higher-temperature plume [*Ito and Clift*, 1998].

[33] Subsidence for Holes 462A and 802A is calculated similarly in Table 2, using eruption depths from CO<sub>2</sub> and reconstructed basement depths that are roughly estimated using the methods of *Ito and Clift* [1998]. The minimum subsidence amounts calculated for Nauru Basin and EMB (3275 and 3775 m) fall within the broad limits (2200 - 4400 m) that are predicted for lithospheric cooling after passage of a plume at 110 Ma [*Ito and Clift*, 1998, Figure 4], and are ~1300 and 1800 m greater than the subsidence amounts calculated above for OJP. (Sediment-based eruption estimates for

OJP of 3000 m [*Saunders et al.*, 1994] provide 2000 - 2700 m greater subsidence for EMB or Nauru compared to OJP). In any case, if OJP was centered on a hotspot swell, it should have subsided more, not less, than the surrounding basins, unless it underwent late stage uplift [*Ito and Clift*, 1998]. In summary, our estimates of shallower eruption depth and greater subsidence reduce the amount but do not eliminate the need for later magmatic activity [*Ito and Clift*, 1998] or other mechanisms [*Neal et al.*, 1997] to account for the anomalously low subsidence of OJP.

### 6.3. Melting and Source Characteristics

[34] For liquids formed by large extents of partial melting, K/Ti is a good indicator of the source's degree of incompatible element enrichment. All of the glasses fall within a narrow range of K/Ti (Figure 4). The source for Hole 807C type A is slightly more enriched, while that for Hole 462A is more depleted and is similar to that from Hole 807C types CG. Glasses from Holes 802A and 803D have intermediate K/Ti in their sources. This order is consistent with previous suggestions for Holes 803D and 807C based on incompatible trace elements [*Mahoney et al.*, 1993a].

[35] Once the variations in source composition are con-

sidered, it is possible to examine differences that may be consistent with variations in the extent and depth of mantle melting. Hole 802A has lower  $\text{Na}_2\text{O}$  at a given MgO than other chemical types (Figure 2); yet it has higher K/Ti (Figure 3) and similar  $\text{K}_2\text{O}$  and  $\text{TiO}_2$  concentrations (Table 2) compared to 807C types CG. These differences cannot be due to differences in crystallization depth. They most likely reflect higher concentrations of K and Ti (and to a lesser extent, Na) in the source of 802A but a greater extent of melting that leads to similar  $\text{K}_2\text{O}$  and  $\text{TiO}_2$  and lower  $\text{Na}_2\text{O}$  at the same MgO in the glasses. Considering that  $\text{Na}_{8,0}$  varies from 3.5 to 1.9% in MORB as the extent of melting increases from 8 to 22% [Klein and Langmuir, 1987], the difference in  $\text{Na}_{8,0}$  between 802A and 807CG (1.81 versus 2.02%) would correspond to roughly 2% (absolute) additional melting. If the total extent of melting is 20%, then this is a 10% (relative) increase in the amount of melting. The difference is probably even larger since the source of 802A probably had a higher  $\text{Na}_2\text{O}$  content. Higher  $\text{SiO}_2$  and lower CaO in Hole 802A glasses [Langmuir *et al.*, 1992; Jaques and Green, 1980], which seems likely for these lavas. If the voluminous lavas of OJP formed by lower extents of melting than the adjacent and less voluminous EMB lavas, then either there must have been much faster or more focussed mantle upwelling beneath OJP, or OJP must have been built over a longer time interval.

### 6.3.1. Source concentrations of $\text{H}_2\text{O}$ and their influence on melting.

[36] Could the relatively high  $\text{H}_2\text{O}$  in the mantle have contributed to the large extent of melting that formed these lavas? If the influence of  $\text{H}_2\text{O}$  on melting was large, then a smaller temperature anomaly would be necessary to account for the large extents of melting. Data from island arc basalts have been used to show that melting increases by ~6% (absolute) for every additional 0.1%  $\text{H}_2\text{O}$  in the source [Stolper and Newman, 1994]. The  $\text{H}_2\text{O}$  content of the sources of the OJP can be calculated after correction for 5065% fractional crystallization (estimated from Figure 2) and 1924% partial melting estimated from  $\text{Na}_{8,0}$  and the range of melting of MORB [Klein and Langmuir, 1987]. Calculated  $\text{H}_2\text{O}$  contents of the mantle source are roughly 250 ppm for EMB and 200300 ppm for OJP lavas (or 300450 ppm if the 3045% crystallization estimates of Neal *et al.* [1997] are used). These  $\text{H}_2\text{O}$  contents are higher than N-MORB sources and are lower than E-MORB sources [Michael, 1995] and more en-

riched Hawaiian sources (525 ppm [Dixon *et al.*, 1997]). The additional  $\text{H}_2\text{O}$  content can account for only ~2% (absolute) of the melting compared to N-MORB. Therefore a substantial temperature anomaly, similar to or greater than that of Iceland is still required. In models of plateau formation and subsidence, larger temperature anomalies result in larger initial excess bathymetry and greater subsequent subsidence. This strengthens arguments that some other process is necessary to account for the small amount of subsidence that OJP has undergone subsequently [Ito and Clift, 1998].  $\text{H}_2\text{O}$  differences in the mantle source are also unable to account for the larger extents of melting of Hole 802A glasses compared to glasses from Hole 807C, since  $\text{H}_2\text{O}$  contents are slightly lower for the source of 802A glasses than for 807C type A glasses.

## 7. Conclusions

[37] For basalts from OJP, NB, and EMB the strong homogeneity of many flow units within each compositionally defined type suggests that each chemical type represents a single eruptive episode with many flow lobes. The homogeneity suggests that magmatic systems (chambers?) were large and well buffered. Magmas at all locations fractionated extensively at shallow pressures. Deep crystallization cannot be ruled out, but it must have been limited, and it cannot account for all of the crystallization. Very high Cl concentrations and Cl/K ratios in all of the glasses suggest that there was abundant hydrothermal activity associated with magmatism and that magmas assimilated hydrothermally influenced material, probably at shallow crustal levels.

[38] Eruption depth at Site 807C derived from  $\text{CO}_2$  and  $\text{H}_2\text{O}$  dissolved in glass is  $1320 \pm 250$  m, which is shallower than previous estimates. It is remotely possible that the magmas erupted far away and flowed long distances to this site. Greater amounts of subsidence are calculated using the shallower eruption depth. This reduces the amount but does not eliminate the need for subsequent magmatism to explain the anomalously shallow nature of the plateau. The shallower eruption estimates also provide support (although weak) for eruption of OJP at or near a MOR. Some of the glasses are oversaturated with  $\text{CO}_2$ , suggesting they did not flow far from their eruptive vent.

[39]  $\text{H}_2\text{O}$  in the mantle source of OJP is similar to the northern MAR source, which is distinctively higher than other MORB sources. The additional  $\text{H}_2\text{O}$  is not

sufficient to have caused extensive melting that generated OJP. A substantial temperature anomaly is still required. EMB liquids formed by the greatest extents of melting. The greater volume of OJP, yet lesser extents of melting compared to EMB means that mantle upwelling beneath OJP was faster or more focused or of longer duration.

## Acknowledgments

[40] We gratefully acknowledge the generous support of this study by the National Science Foundation, grant OCE 95 04941, to Peter Michael and Winton Cornell. Clive Neal generously provided glass chips from Malaita Island. Winton Cornell assisted with the major element and Cl analyses. Discussions with John Mahoney, Garrett Ito, Jackie Dixon, John Tarduno, Clive Neal, Pat Castillo, Peter Hooper, and Steven Self helped develop the ideas in this paper. Jackie Dixon generously provided a sample of degassed glass for the CO<sub>2</sub> analyses and ran some glasses by FTIR for interlab comparisons. Thoughtful and constructive reviews by Garrett Ito, Jackie Dixon, and M. Tejada improved the paper. The assistance and support and samples of the Deep Sea Drilling Program and Ocean Drilling Program, including their core repositories and curating staff, are gratefully acknowledged.

## References

- Batiza, R., Trace element characteristics of Leg 61 basalts, in *Initial Reports of the Deep Sea Drilling Project*, vol. 61, edited by R. Larson et al., pp. 689-695, U.S. Gov. Print. Off., Washington, D. C., 1981.
- Bercovici, D., and J. J. Mahoney, Double flood basalts and plume head separation at the 660-kilometer discontinuity, *Science*, *266*, 1367-1369, 1994.
- Campbell, I. H., and R. W. Griffiths, Implications of mantle plume structure for the evolution of flood basalts, *Earth Planet. Sci. Lett.*, *99*, 79-93, 1990.
- Castillo, P. R., R. Batiza, and R. Stern, Petrology and geochemistry of Nauru Basin igneous complex: Large-volume, off-ridge eruptions of MORB-like basalt during the Cretaceous, *Initial Rep. Deep Sea Drill. Proj.*, *89*, 555-576, 1986.
- Castillo, P. R., R. W. Carlson, and R. Batiza, Origin of Nauru Basin igneous complex: Sr, Nd and Pb isotope and REE constraints, *Earth Planet. Sci. Lett.*, *103*, 200-213, 1991.
- Castillo, P. R., M. S. Pringle, and R. W. Carlson, East Mariana Basin tholeiites: Cretaceous intraplate basalts or rift basalts related to the Ontong Java plume?, *Earth Planet. Sci. Lett.*, *123*, 139-154, 1994.
- Coffin, M. F., and O. Eldholm, Large igneous provinces: Crustal structure, dimensions, and external consequences, *Rev. Geophys.*, *32*, 1-36, 1994.
- Coffin, M. F., and L. M. Gahagan, Ontong Java and Kerguelen Plateaux: Cretaceous Iceland's?, *J. Geol. Soc.*, *152*, Part 6, 1047-1052, 1995.
- Danyushvesky, L. V., A. V. Sobolev, and L. V. Dmitriev, Estimation of the pressure of crystallization and H<sub>2</sub>O content of MORB glasses: Calibration of an empirical technique, *Mineral. Petrol.*, *57*, 185-204, 1996.
- Devey, C. W., C.-D. Garbe-Schönberg, P. Stoffers, C. Chauvel, and D. F. Mertz, Geochemical effects of dynamic melting beneath ridges: Reconciling major and trace element variations in Kolbeinsey (and global) mid-ocean ridge basalt, *J. Geophys. Res.*, *99*, 9077-9095, 1994.
- Dixon, J. E., E. Stolper, and J. R. Delaney, Infrared spectroscopic measurements of CO<sub>2</sub> and H<sub>2</sub>O in Juan de Fuca Ridge basaltic glasses, *Earth Planet. Sci. Lett.*, *90*, 87-104, 1988.
- Dixon, J. E., D. A. Clague, and E. M. Stolper, Degassing history of water sulfur and carbon in submarine lavas from Kilauea volcano, Hawaii, *J. Geol.*, *99*, 371-394, 1991.
- Dixon, J. E., E. M. Stolper, and J. R. Holloway, An experimental study of water and carbon dioxide solubilities in mid-ocean ridge basaltic liquids, part I, Calibration and solubility models, *J. Petrol.*, *36*, 1607-1631, 1995.
- Dixon, J. E., D. A. Clague, P. W. Wallace, and R. Poreda, Volatiles in alkalic basalts from the North Arch Volcanic Field, Hawaii: Extensive degassing of deep submarine-erupted alkalic series lavas, *J. Petrol.*, *38*, 911-939, 1997.
- Farnetani, C. G., M. A. Richards, and M. S. Ghiorso, Petrological models of magma evolution and deep crustal structure beneath hotspots and flood basalt provinces, *Earth Planet. Sci. Lett.*, *143*, 81-96, 1996.
- Fine, G., and E. Stolper, CO<sub>2</sub> in basaltic glasses: Concentration and speciation, *Earth Planet. Sci. Lett.*, *76*, 263-278, 1986.
- Fisk, M. R., A. W. McNeill, D. A. H. Teagle, H. Furnes, and W. Bach, Data report: Major element chemistry of Hole 896A glass, in *Proceedings of the Ocean Drilling Program, Scientific Results*, 148, edited by J. C. Alt et al., pp. 3-22, Ocean Drill. Program, College Station, Tex., 1996.
- Gladczenko, T. P., M. F. Coffin, and O. Eldholm, Crustal structure of Ontong Java Plateau: Modeling of new gravity and existing seismic data, *J. Geophys. Res.*, *102*, 22,711-22,729, 1997.
- Hooper, P. R., The Columbia River Flood Basalt Province: Current status, in *Large Igneous Provinces: Continental, Oceanic and Planetary Flood Volcanism, Geophys. Monogr. Ser.*, vol. 100, edited by J. J. Mahoney and M. F. Coffin, pp. 1-28, AGU, Washington, D. C., 1997.

- Ito, G., and P. D. Clift, Subsidence and growth of Pacific Cretaceous Plateaus, *Earth Planet. Sci. Lett.*, *161*, 85-100, 1998.
- Jambon, A., B. Déruelle, G. Dreibus, and F. ineau, Chlorine and bromine abundance in MORB: The contrasting behaviour of the Mid-Atlantic Ridge and East Pacific Rise and implications for chlorine geodynamic cycle, *Chem. Geol.*, *126*, 101-117, 1995.
- Jaques, A. L., and D. H. Green, Anhydrous melting of peridotite at 0-15 kb pressure and the genesis of tholeiitic basalts, *Contrib. Mineral. Petrol.*, *73*, 287-310, 1980.
- Klein, E. M., and C. H. Langmuir, Global correlations of ocean ridge basalt chemistry with axial depth and crustal thickness, *J. Geophys. Res.*, *92*, 1987, 8089-8115.
- Kroenke, L. Geology of the Ontong Java Plateau, 119 p., Ph.D. thesis, Univ. of Hawaii, Honolulu, 1972.
- Kroenke, L. W., et al., *Proceedings of Ocean Drilling Program, Initial Reports*, vol. 130, U.S. Gov. Print. Off., Washington, D.C., 1991.
- Langmuir, C. H., E. M. Klein, and T. Plank, Petrological systematics of mid-ocean ridge basalts: Constraints on melt generation beneath ocean ridges, in *Mantle Flow and Melt Generation at Mid-ocean Ridges*, *Geophys. Monogr. Ser.*, vol. 71, edited by J. Phipps Morgan, D. K. Blackman, and J. M. Sinton, pp. 183-280, AGU, Washington, D. C., 1992.
- Larson, R. L., Geological consequences of super plumes, *Geology*, *19*, 963-966, 1991.
- Mahoney, J.J., An isotopic survey of Pacific oceanic plateaus: Implications for their nature and origin, in *Seamounts, Islands and Atolls*, *Geophys. Monogr. Ser.*, vol. 43, edited by B. Keating et al., pp. 207-220, AGU, Washington, D. C., 1987.
- Mahoney, J. J., and K. J. Spencer, Isotopic evidence for the origin of the Manihiki and Ontong Java oceanic plateaus, *Earth Planet. Sci. Lett.*, *104*, 196-210, 1991.
- Mahoney, J. J., M. Storey, R. A. Duncan, K. J. Spencer, and M. Pringle, Geochemistry and age of the Ontong Java Plateau, in *The Mesozoic Pacific: Geology, Tectonics and Volcanism*, *Geophys. Monogr. Ser.*, vol. 77, edited by M.S. Pringle et al., pp. 233-262, AGU, Washington, D. C., 1993a.
- Mahoney, J. J., M. Storey, R. A. Duncan, K. J. Spencer, and M. Pringle, Geochemistry and geochronology of Leg 130 basement lavas: Nature and origin of the Ontong Java Plateau, in *Proceedings of the Ocean Drilling Program, Scientific Results*, vol. 130, edited by W. H. Berger, L. W. Kroenke, and L. A. Mayer, pp. 3-22, Ocean Drill. Program, College Station, Tex., 1993b.
- Michael, P. J., Regionally distinctive sources of depleted MORB: Evidence from trace elements and H<sub>2</sub>O, *Earth Planet. Sci. Lett.*, *131*, 301-320, 1995.
- Michael, P. J., and J.-G. Schilling, Chlorine in mid-ocean ridge magmas: Evidence for assimilation of seawater-influenced components, *Geochim. Cosmochim. Acta.*, *53*, 3131-3143, 1989.
- Michael, P. J., and W. C. Cornell, influence of spreading rate and magma supply on crystallization and assimilation beneath mid-ocean ridges: Evidence from chlorine and major element chemistry of mid-ocean ridge basalts, *J. Geophys. Res.*, *103*, 18,325-18,356, 1998.
- Michael, P. J., R. L. Chase, and J. F. Allan, Petrologic and geologic variations along the Southern Explorer Ridge, northeast Pacific Ocean, *J. Geophys. Res.*, *94*, 13,895-13,918, 1989.
- Nakanishi, M., K. Tamaki, and K. Kobayashi, A new Mesozoic isochron chart of the northwest Pacific Ocean: Paleomagnetic and tectonic implications, *Geophys. Res. Lett.*, *19*, 693-696, 1992.
- Neal, C.R., J. J. Mahoney, L. W. Kroenke, R. A. Duncan, and M. G. Pettersen, The Ontong Java Plateau, in *Large Igneous Provinces: Continental, Oceanic and Planetary Flood Volcanism*, *Geophys. Monogr. Ser.*, vol. 100, edited by J. J. Mahoney and M. F. Coffin, pp. 183-216, AGU, Washington, D. C., 1997.
- Richards, M. A., D. L. Jones, R. A. Duncan, and D. J. DePaolo, A mantle plume initiation model for the Wrangelia flood basalt and other oceanic plateaus, *Science*, *254*, 263-267, 1991.
- Saunders, A. D., Geochemistry of basalt from the Nauru Basin, Deep Sea Drilling Project Legs 61 and 89: Implications for the origin of oceanic flood basalts, in *Initial Reports of the Deep Sea Drilling Project*, vol. 89, edited by R. Moberly et al., pp. 499-518, U.S. Govt. Print. Off., Washington, D. C., 1986.
- Saunders, A. L., T. L. Babbs, M. J. Norry, M. G. Pettersen, B. A. McGrail, J. J. Mahoney, and C. R. Neal, Depth of emplacement of oceanic plateau basaltic lavas, Ontong Java Plateau and Malaita, Solomon Islands: Implications for the formation of LIPs? (abstract), *Eos Trans. AGU*, *74*, 552, 1994.
- Self, S. S., T. Thordarson, and L. Keszthelyi, Emplacement of continental flood basalt lava flows, in *Large Igneous Provinces: Continental, Oceanic and Planetary Flood Volcanism*, *Geophys. Monogr. Ser.*, vol. 100, edited by J. J. Mahoney and M. F. Coffin, pp. 381-410, AGU, Washington, D. C., 1997.
- Sliter, W. V., and R. M. Leckie, Cretaceous planktonic foraminifers and depositional environments from the Ontong Java Plateau with emphasis on Sites 803 and 807, in *Proc. Ocean Drill. Program, Sci. Results*, *130*, 63-84, 1993.
- Stolper, E., The speciation of water in silicate melts, *Geochim. Cosmochim. Acta.*, *46*, 2609-2620, 1982.
- Stolper, E. M., and S. Newman, The role of water in the petrogenesis of Mariana Trough magmas, *Earth Planet. Sci. Lett.*, *121*, 293-325, 1994.
- Storey, M., J. J. Mahoney, L. W. Kroenke, and A. D. Saunders, Are oceanic plateaus sites of komatiite formation?, *Geology*, *19*, 376-379, 1991.





- Tarduno, J. A., W. V. Sliter, L. Kroenke, M. Leckie, H. Mayer, J. J. Mahoney, R. Musgrave, M. Storey, and E. L. Winterer, Rapid formation of Ontong Java Plateau by Aptian mantle plume volcanism, *Science*, 254, 399-403, 1991.
- Tejada, M. L. G., J. J. Mahoney, R. A. Duncan, and M. P. Hawkins, Age and geochemistry of basement and alkalic rocks of Malaita and Santa Isabel, Solomon Islands, southern margin of Ontong Java Plateau, *J. Petrol.*, 37, 361-394, 1996.
- Weaver, J. S., and C. Langmuir, Calculation of phase equilibrium in mineral-melt systems, *Comput. Geosci.*, 16, 1-19, 1990.
- Webster, J. D., R. J. Kinzler, and E. A. Mathez, Chloride and water solubility in basalt and andesite melts and implications for magmatic degassing, *Geochim. Cosmochim. Acta.*, 63, 729-738, 1999.
- White, R. S., and D. Mckenzie, Mantle plumes and flood basalts, *J. Geophys. Res.*, 100, 17,543-17,585, 1995.
- Yang, H.-J., R. L. Kinzler, and T. L. Grove, Experiments and models of anhydrous, basaltic olivine-plagioclase-augite saturated melts from 0.001 to 10 kbar, *Contrib. Mineral. Petrol.*, 124, 1-18, 1996.